INTERNATIONAL DESIGN CONFERENCE - DESIGN 2016
Dubrovnik - Croatia, May 16 - 19, 2016.

INTRODUCING SELECTIVE LASER MELTING TO MANUFACTURE MACHINE ELEMENTS

R. Lachmayer, Y. A. Zghair, C. Klose and F. Nürnberger

Keywords: machine element, additive manufacturing, lightweight design

1. Introduction

Manufacturing processes are aiming to deliver new customized products more quickly and cost effective. Increasing manufacturing flexibility is a key strategy for efficiently improving market responsiveness in the face of uncertain future product demands. Complexity of products being manufactured today is increasing, observable at the number of parts being used in devices and the developed performance or operation. Being able to build different types of products in one production facility will certainly shorten the manufacturing processes. Casting, forging, extrusion, powder metallurgy (P/M) etc., are considered traditional manufacturing processes, where each part may pass through more than one of these processes to reach the final required geometry, mechanical and chemical properties [Shen et al. 2006].

Additive Manufacturing (AM) is considered one of the most modern production processes. It enables the fabrication of component geometries with decreased time to market, near net shape production, a high material utilization rate, high flexibility in production, and geometrical freedom for complex parts or those, that cannot be realized using conventional techniques [Olakanmia et al. 2015].

Among diverse established AM technologies, Selective Laser Melting/Sintering (SLM/SLS) has become a promising manufacturing route for engineering parts. Direct Metal Laser Sintering (DMLS) is a rapid manufacturing technique derived from SLM. It enables prompt modeling of metal objects with defined structure and shape of complex geometry on the basis of virtual 3D model data. It is considered one of the best manufacturing techniques in laser sintering due to its great potentiality in direct manufacturing [Capello et al. 2005]. In addition, it is possible to work with wide range of materials with high precision and for complex geometries.

Introducing SLM in commercial production of machine elements is a big challenge. Amongst others, limited understanding of the material properties, limited size of the produced parts, surface tribology and dynamic properties are some points that prevent this technology to be used over the traditional methods. But on the other hand there are many advantages that might make it a promising method in machine elements manufacturing, such as:

- Functional integration. Improved functionality by AM offers a clear advantage for the ability to add functions to the produced part directly without or with less need for further components, tooling or assembly processes. This will help in almost direct and complete part production with less assembly time and greater functionality and flexibility.
- To improve quality control through high machine accuracy capabilities and thence reduce scrap, rework, and conventional inspection.

- To achieve greater densities with inhomogeneous distribution according to pre-set up configuration with the ability to build hollow components with internal structures to help in strengthen the part body with less weight and cost by saving material [Lachmayer et al. 2016].
- Time and cost effective building of complex parts or those parts that require a lot of machining. This is done by reducing of manufacturing time, elimination of tooling to reach the final geometry especially for materials that are not easy to machine without the need for some post processes, with minimum finishing and the cost of material consumed if compared with the subtractive manufacturing methods.
- Low harmful emissions.
- Can be used for rapid prototyping, component manufacturing, repair jobs and hybrid material components manufacturing [Lachmayer et al. 2016].

For a fully or partially contribution of SLM technologies within machine elements manufacturing, a validation has to be carried out and cost-effectiveness of the processing as well as technical enhancement over the traditional methods has to be proved. Therefore, this work starts as a first step towards testing materials and to identify the suitability of manufacturing machine elements. Further steps are to improve the functionality of parts manufactured by developing a new concept to build one body with a closed surface but some internal hollow space with internal enforce structures by using SLM. The challenge is to prevent the powder from entering the inside, and to proof the possibility to manufacture internal structures with different precise geometries. This will open the door for future applications to manufacture parts with high functionality, reduced weight and good mechanical properties. Finally, this work aims to present the ability to print on precast material and additional internal structures. This will allow to produce hybrid components which are composed of different parts and materials according to application requirements. All building processes are carried out by using an EOS M280 machine [EOS 2010].

2. Multi-phase building approach to build hollow bodies

In this paper, a new approach is introduced to design and manufacture hollow bodies from one and/or two metal alloys, connected together by means of SLM, with dividing the building process to more than one building phase. The approach will introduce new variables to the design process, such as: the ability to reduce the weight of solid parts by making them hollow, so that the designer will be more flexible in the design of light weight parts, or design inhomogeneous parts having solid and hollow volumes. Increase the possibility to integrate more functions to the part and design more complex geometries.
The approach idea based on the ability of 3D metal printing machines to sinter metal alloy powder on another part build from the same or different metal alloy, but from the same base metal. Therefore, it possible to use this machines advantage to build hollow parts as follows:

- Prepare a CAD model for the hollow part with one face opened, and make sure that the face covers the whole cavities of the part to be possible later to clean it from powder.
- Load the CAD model to the 3D printing machine, and let the open face oriented to the up direction.
- After completing the first building process, take out the part and clean it from metal powder.
- Prepare a suitable insert to cover the open face of the part. This insert must be from the same powder metal alloy, or from another alloy have a good cohesion with the sintered powder. Make sure the insert is thick enough and fixed so that it will not bend during the process.
- Prepare another CAD model to complete the remaining upper volume of the part. This model must be solid and cover both the upper face walls of the part, and also the complete face of the insert.
- Put the part again in the machine, fix it, and complete the building process Figure 1.

The designer must take in consideration the possibility to divide the building process to more than two phases in case that the part has more than one cavity, and it is not possible to take out the metal powder from one hole. The upper surface of the part walls must be wide enough to insure good contact with the volume that will be printed over it later. This surface must always be plane, because the SLM technique is to build on plane surfaces only.

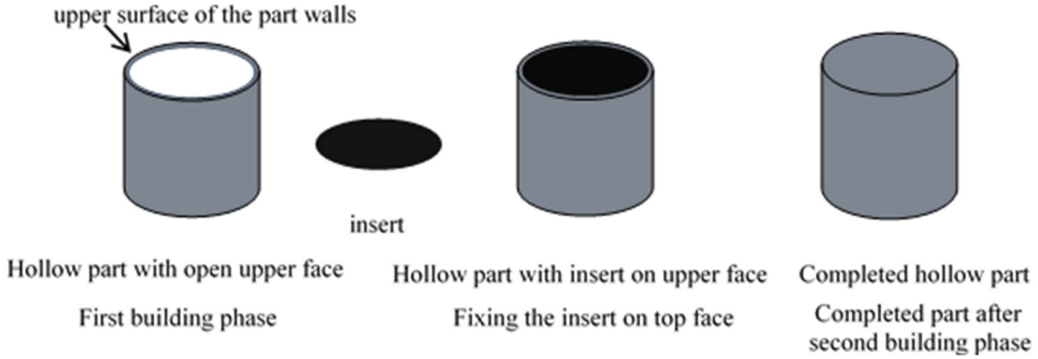

Figure 1. Manufacturing steps of hallow parts

3. Variables for SLM

The SLM process is affected by many parameters and material variables which influencing the processing and densification mechanism of sintered parts. These parameters have direct effect on the part geometry, size, density, and spatial distribution of pores within a component. Such information is essential in developing strategies for reducing the defect content inside parts especially the pores and its location. This is because pores play a big role in reducing the density of built part, and its location near the part surface is more unlikable than in the core, due to its negative effect in fractures. So, good understanding of the connection between these parameters will help to produce denser products with low pores. Table 1 shows a list of some SLM process parameters and material variables with different values ranges for different materials and machines power [Agarwala et al. 1995], [Murali et al. 2003], [Simchi and Pohl 2003, 2004], [Kruth et al. 2005], [Shen et al. 2006], [Manfredi et al. 2014]. This table will be the guide through this analysis to select the suitable values of the machine parameters during the printing process and give an idea how these values affect the quality of produced component.

To understand how the laser power and mirror speed are adjusted during the printing process in the later part of this analysis, Equation (1) below is used to define the specific laser energy input ψ and the laser power is determined as below [Olakanmi 2013], [Tammas-Williams et al. 2015]:

$$\psi = \frac{P}{uhd} \quad \text{[Simchi and Pohl 2004]} \tag{1}$$

Where: ψ is laser intensity per volume (J/mm^3), P is the laser power (W), u is the scan rate (mm/s), h is the scan spacing (mm) and d is the layer thickness (mm).

The above equation correlates the local volume heat input with scanning speed, power and offset between melt paths. Increasing the laser power and reducing the mirror speed will increase the part density [Olakanmi 2013], but this will help to agglomerate the powder and balling phenomenon will appear very clearly. Therefore, in this work the laser power is set to the recommended machine parameters when printing AlSi10Mg powder, but these parameters are adjusted when printing over a another cast material, and Equation (1) is used to estimate the new parameters set (more information about how to select the parameters are given in the experimental section of this work). The employed melt or scanning strategy also has an effect on the amount of energy exposed by laser on each layer. The melted zone diameter usually is larger than the laser spot diameter (which will be noticed later in microscopic examination), therefore, Beam Offset (BO) correction value is used by DMLS process to make sure that the contour of part will correspond exactly to CAD model [Manfredi et al. 2014] Figure 2.

Figure 3 shows the difference in roughness between the (as built) and machined specimens which are used in this analysis. The micro cracks of unmachined fractured specimen surface plays a big role in crack initiation and part failure [Kasperovich and Hausmann 2015]. Therefore, machining the surface will enhance the mechanical properties and remove these surface cracks. Another surface treatment that can be used to enhance the surface roughness is shot peening, where the roughness can be reduced to 85% with a pressure of 8 bar [Manfredi et al. 2014].

Table 1. SLS/SLM process parameters and material variables influencing the processing and densification mechanism of fabricated parts

Parameter	Value	Effect
Laser power	From 20 to 400 watt Depending on machine type.	12-16 J/mm2 considered the threshold between SLS/SLM.
Laser type	CO2, lamp or diode pumped, disk or fibre.	
Scanning speed	20 – 1500 mm/sec.	Process speed and balling phenomenon.
Scan spacing	0.1, 0.15, 0.2 mm, depending on material powder.	Process speed, fusing/unfused areas.
Scanning strategy	Sky writing, hatch pattern, up-skin and down-skin.	Density and surface hardness.
Layer thickness	20 – 150 µm [Agarwala et al. 1995]	Thick: no optimal adhesion between layers (affect melting depth)/ thin: tearing –off structure during recoating (struck with recoater) [Manfredi et al. 2014].
Spot size	0.1 – 0.25 mm.	
Powder grains size	20-75 µm.	Have an effect on porosity size.
Deposit method	Scraper / roller.	
Powder properties	Thermal expansion, oxide content and distribution, laser absorption, chemical properties, composition, surface tension, viscosity & fluidity and heat conductivity.	Pores, mechanical properties.
Atmosphere	Argon (Ar) / Nitrogen (N2).	Chemical interaction.
Pre-process	Heating up the platform or not.	Reduce the humidity, sintered part stresses and required laser power.
Post process	Heat treatment, hot isostatic pressing, … etc.	Relieving residual stresses, increasing the density of product and improving mechanical properties.
Surface condition	Sand blasting, shot peening and machining.	Surface density, surface cracks and hardness.

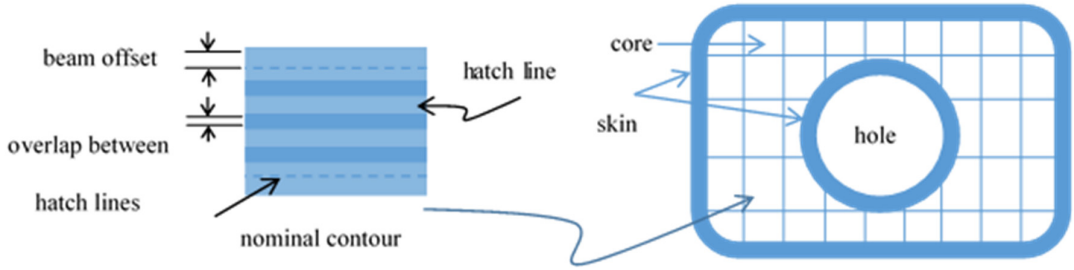

Figure 2. Laser exposure

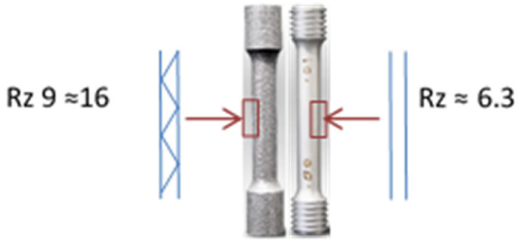

Figure 3. As built' (left) and 'machined' (right) test specimens to be used in tensile test

4. Experimental section

4.1 Material

Aluminum (Al) alloys are considered one of the most used metals in industry and it comes in the second place after steel; there are heat treatable and non-heat treatable alloys [Olakanmia et al. 2015]. In this experiment, AlSi10Mg material is used, which is an optimized aluminum alloy powder for processing on EOSINT M systems. Full details for the alloy specification can be found in the material data sheet issued by EOS [2011].

4.2 Tensile test specimen preparations

4.2.1 Full specimen in one-phase building (one metal)

To prepare tensile test specimens for this experiment, a CAD model according to DIN 50125 standards is used. The platform of the machine is heated up to 200 °C, the chamber room is filled with nitrogen gas, then the laser parameters are set to a laser power of 370 W, mirror speed of 1,300 mm/s, distance of 0.19 mm and layer thickness is 0.03 mm. The building process is started to produce a set of four pieces of specimens with different alignment directions on the platform as shown in Figure 4 (a), this will help to test and find the difference in mechanical properties for each building position.

4.2.2 Full specimen in two-phase building (one metal)

In this experiment, another building process is started to build a set of specimens with half lengths. The printing process is repeated in the same alignment positions as in the one-phase building. After completing the building process, these half specimens are machined, prepared and fixed again to the platform of the machine to be ready for the second building phase Figure 4 (b). The second half of the specimens will be built up in the z-direction only, which means that four combinations of building direction specimens, (x-z, y-z, xy-z, and z-z), will be obtained. The laser parameters are adjusted for the first building layers (which is in normal building considered as lower skin) because the process is to print directly on the platform (which is in this case the half specimen upper surface) and no support structure will be used. The laser power is 370 W, mirror speed is 1,300 mm/s, distance is 0.19 mm and layer thickness is 0.03 mm.
After the second building process is completed Figure 4 (c), the full length specimens are machined to the final size to be ready for the tensile test.

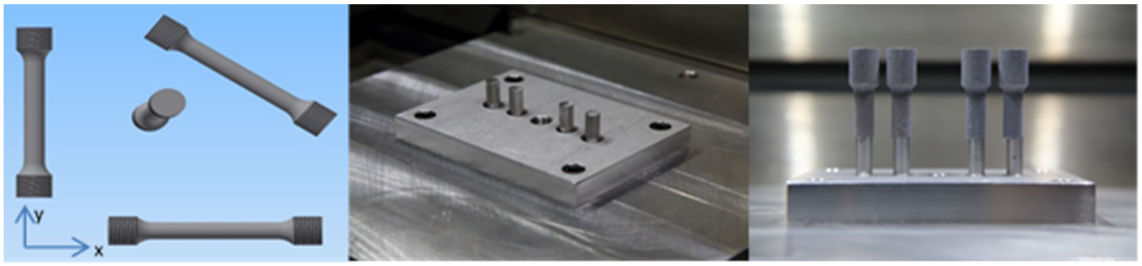

Figure 4. Specimens building steps: (a) full length CAD model of the specimen's orientations on the building platform, (b) the prepared half specimens inside the machine, (c) the half specimens after building process is completed (two stage printing)

4.2.3 Full specimen in two-phase building (two metals)

This experiment is very similar to the two-phase building process, but the first part is from a different cast (not sintered) Al alloy. The first halves of the specimens are machined according to the dimensions of the DIN 50125 standard, then it is fixed on the machine platform. The platform is heated up to 200 °C, and the chamber room filled with nitrogen gas. The laser parameters are also adjusted for the first building layers (lower skin), no support structure will be used, and the upper surface of the specimens

is considered the platform. The laser power is 370 W, mirror speed is 1100 mm/s, distance is 0.19 mm and layer thickness is 0.03 mm.

5. Results

5.1 X-Ray tests

After manufacturing and machining the specimens, X-ray computed tomography (CT) was applied to investigate whether there are defects in the specimens which were manufactured in two stages (AlSi10Mg powder only). The measurements were performed using a nominal spatial resolution of 10 µm, an acceleration voltage of 70 kV and and an image integration time of 600 ms. The investigated area is the cross section (diameter 10 mm) in the middle of each specimen, Figure 5. The examined cross sections show no evidence of increased porosity, cracks or other defects except for a few local spots with an increased density. This verifies that the manufactured material and the contact surfaces of the two printed halves are well melted together and feature a very low porosity. On the here investigated length scale, no evidence of a weakened cross section which could propagate fracture due to mechanical loading, is present.

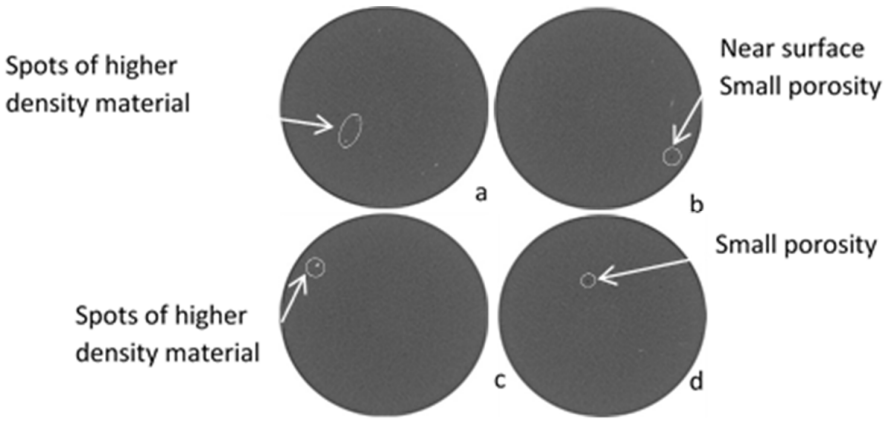

Figure 5. X-Ray scans for some selected slices through the two-phase printed specimens: (a) x direction printed, (b) y direction printed, (c) xy direction printed, (d) z direction printed

5.2 Tensile tests

The specimens which were manufactured by the one- and two-phase building process (AlSi10Mg powder only) were heated up to 300 °C for two hours to relief residual stresses. Subsequently, tensile tests were performed at room temperature according to DIN EN 6892-1 B to determine the mechanical properties and to investigate both the fracture position and the fractured surface. Figure 6 (a) depicts the fracture shape (cup-cone fracture) and the fracture position, which in some cases is not within the gauge length GL. No fracture occurred in the contact area (biplane) in the centre of the four specimens that were manufactured in two-stages (cf. Table 2). The tensile strength of the specimens which were built under nitrogen atmosphere is lower than the tensile strength for specimens manufactured using Argon due to aluminum nitrides formed during melting in the nitrogen atmosphere [Kruth et al. 2005]. In general, the elongation at fracture in specimens printed in z direction is lower than for specimens printed in x, y and xy directions. This can be observed for both printing processes (one and two-stage). The area reduction for the specimens in z direction for both one and two-stage specimens is less than the for the other specimensFor the specimens manufactured in the two-phase building process, and the cast basic structure, the tensile tests show that the fracture occurs in the cast part of the specimen Figure 6 (b). This is due to an increased strength of the sintered alloy in comparison to the cast alloy, in addition the interface shows a very good bonding between the two segments without any fracture.

Table 2. Tensile test results (GL: gauge length)

Specimen No.	Orientation on platform/Printing stages	F Max kN	Strength MPa	Elongation %	Area reduction %	Fracture position
specimen in one-phase building (powder only)						
1	xy oriented/ 2- phases	7.55	272	10.2	40	out-GL
2	y oriented/ 2- phases	7.29	263	9.1	40	out-GL
3	x oriented/ 2- phases	7.41	269	8.5	36	out-GL
4	z oriented/ 2- phases	7.65	278	8.1	30	out-GL
specimen in two-phase building (powder only)						
5	z oriented/ 1- phases	7.36	269	6.2	33	out-GL
6	x oriented/ 1- phases	7.51	268	16.3	41	in-GL
7	xy oriented/ 1- phases	7.62	270	17.7	39	in-GL
8	y oriented/1- phases	7.23	261	7.9	39	out-GL
specimen in two-phase building (cast basic structure and powder)						
9	cast/2-phases	-	-	13.4	-	in-GL

Figure 6. Fracture type and position of a specimen (powder only) (b) Fracture type and position of a specimen (cast basic structure and powder)

5.3 Fractographic analysis

After the tensile test the fractured surfaces of all specimens (except the two-phase specimens with the cast basic structure) were examined to investigate whether there are any unusual findings. The x, y, and xy specimens show no unexpected behaviour; no unmelted powder or increased porosity is present which might cause a crack propagation Figure 7 (a, b, c, f, g, h). Figure 7 (d, e) shows another fracture type with many uniform lines in various directions. Each set of these lines is present in a different layer and the angle between these lines is 67 degrees, which corresponds to the angle that the laser beam rotates after each printing layer.

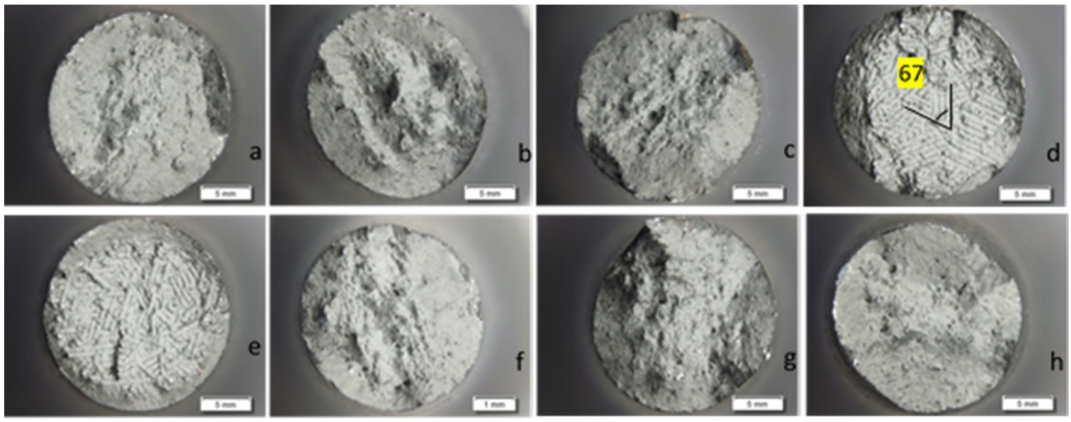

Figure 7. Fractographic photos for the fracture surface of the specimens (one and two-stage printing): (a, b, c, f, g, h) x, y, xy, z direction printing alignment for both one and two-stage printing, (d, e) z direction printing alignment for both one and two-stage printing

This visualizes how the laser is sintering the metal powder in paths, with an overlapping of each path to the next one. The fracture occurs between the agglomerated sintered powder particles layers, and this not the case in the other printing directions. Anyway, these two specimens which are printed in the vertical position show a reduced elongation at fracture but almost keep the tensile strength.

5.4 Microscopic analysis

A microscopic examination is carried out regarding the interface between the sintered part and the subsequently added sintered part as well as for the cast part and the added sintered part.
In the first case homogeneity between the original and the added parts can be observed; no separation at the interface is present, cf. Figure 8 (a). In the second case the laser melts both the powder and the previously cast material thus forming the interface; the difference in colours is due to the different chemical compositions of the aluminum alloys used in this experiment. It can be noticed that the surface features a bigger crescent than the other layers due to a higher energy applied to sinter the surface regarding a better finish, cf. Figure 8 (b).

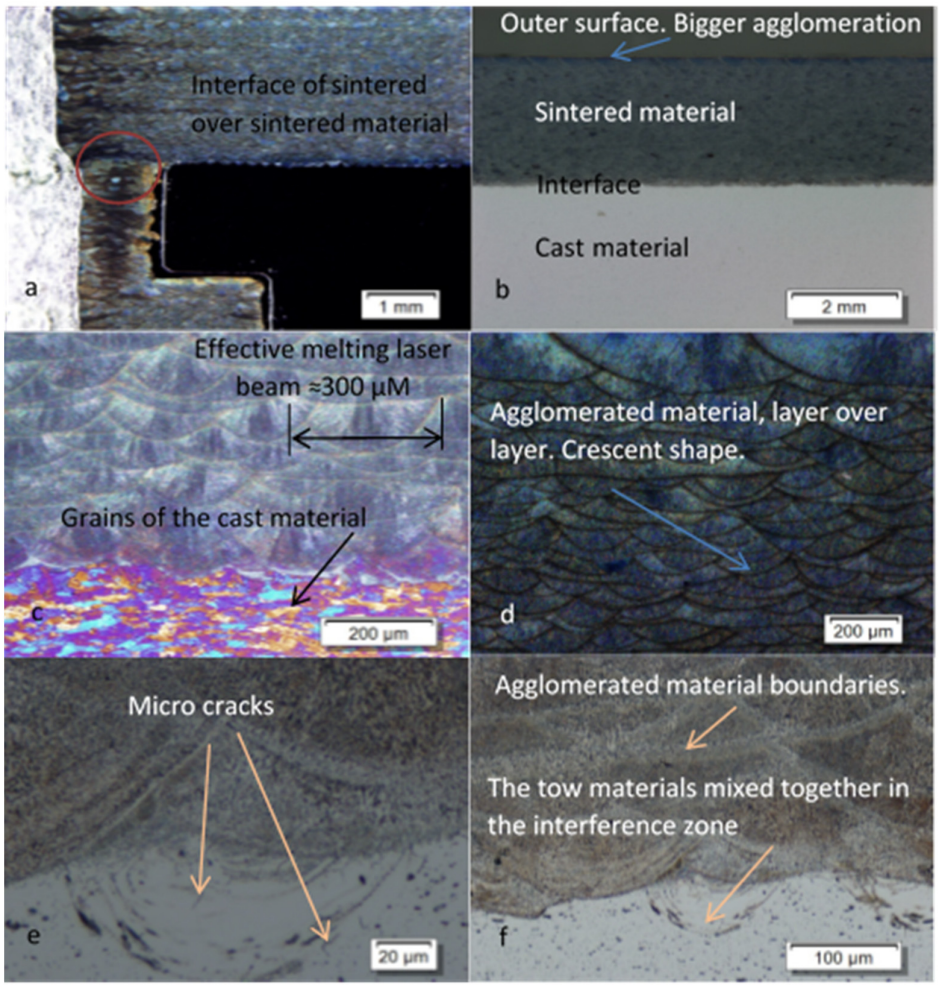

Figure 8. Micrographs of the interface zone of sintered part built over sintered part or cast part, respectively: (a) Interface of sintered material over sintered material (etching: mixture of sulfuric acid and hydrofluoric acid), (b) Interface zone of sintered material over cast material (etching: mixture of sulfuric acid and hydrofluoric acid), (c, d) Agglomerated material and the crescent shapes of the melting pools (etching: Barker (c) and mixture of sulfuric acid and hydrofluoric acid (d)), (e, f) interface zone and micro cracks (etching: mixture of sulfuric acid and hydrofluoric acid)

Furthermore, it can be observed that the geometry of each single melting pool has a crescent shape. The distance between each of these is about 300 µm, while the pre-set value for the laser distance is 190 µm. This deviation is caused due to the effective laser diameter, and explains the overlap of the melting pools, cf. Figure 8 (c, d). In the interface zone some few micro cracks present, cf. Figure 8 (e), though in general it can be noticed that the laser melts the cast metal up to a sufficient depth resulting in a homogenous mixture of both metals, cf. Figure 8 (f).

6. Future applications

6.1 Hollow gear with internal structure

To verify the multi-phase building approach of creating bodies from a three dimensional CAD models to substitute or modify existing parts experiments at the example of a hollow gear are carried out. The main idea is to manufacture a hollow gear sintered by an EOS machine with SLM technology while preventing any powder of getting inside. Therefore, the process is divided into two phases: printing the gear with one face opened, subsequently putting a suitable insert on the top face after removing the powder out of the gear, and finally complete printing of the upper face.
First, the CAD model of a gear with one open side to the upper direction is prepared with a random internal geometric structure. The platform is heated up to 200 °C, the chamber filled with nitrogen gas, the machine parameters set up with a laser power of 370 watt, scanning speed is 1,300 mm/s, offset 0.19 mm, laser spot 0.02 mm and a strip overlap of 0.02 mm. After the sintering process is completed, the gear is removed and cleaned inside, cf. Figure 9 (a). The gear is then capped with a suitable aluminum plate (machined to fit with the structure's upper edges) to prevent powder from inserting during the next printing stage, Figure 9 (b). Fixing the gear model inside the printing platform and covering the whole surrounding with powder, the laser parameters are selected according to Table 1, Equation (1) and Table 3.

Table 3. 3-D laser printer parameters set-up

	Laser intensity ψ J/mm^3	Laser Power W	Scanning Speed mm/s	Distance mm	Strips overlap mm
Lower skin/first layer on cut surface	59	370	1,100	0.19	0.02
Lower and upper skin / rest of layers	132	370	775	0.12	0.03
Strips	50	370	1,300	0.19	0.02

The second printing stage over the upper area of the gear is then started. After completing the printing process, a side cut of the gear is made as shown in Figure 9 (c) to make sure that the process completed successfully as planned and to take samples from the interface between the sintered material and the covering sheet for examinations and to make sure that the upper edges of the internal structure are in a good connection with the upper face.

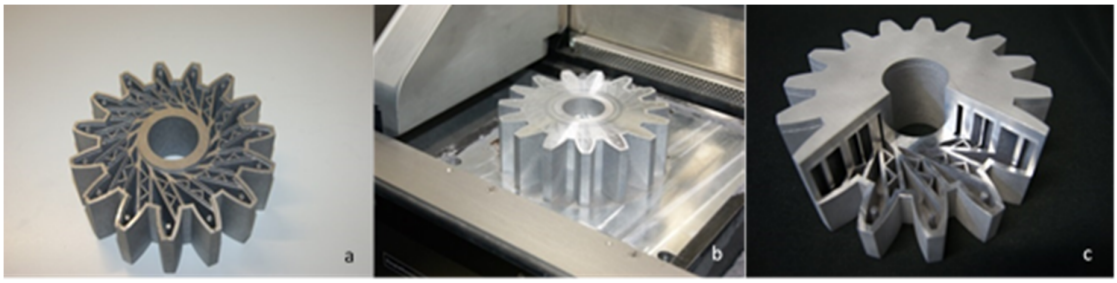

Figure 9. Building process of hollow gear: (a) first stage completed, (b) capping model (inside the printer), (c) side cut in the gear model after completion

6.2 Hybrid material hollow shaft manufacturing

Additionally, the process used to manufacturing the gear was applied to manufacture a shaft from two different aluminum alloys. The first half of the shaft is from a common aluminum cast alloy. The CAD model with all required details was prepared, then the machined part of the shaft fixed to the platform and the machine platform heated up. The laser parameters are set up according to Table 3, the chamber room is filled with nitrogen and the printing process is started. The final result is a shaft with an integrated gearing at the end, two segments of different materials and thus mechanical properties, reduced weight and some internal supporting structure, Figure 10.

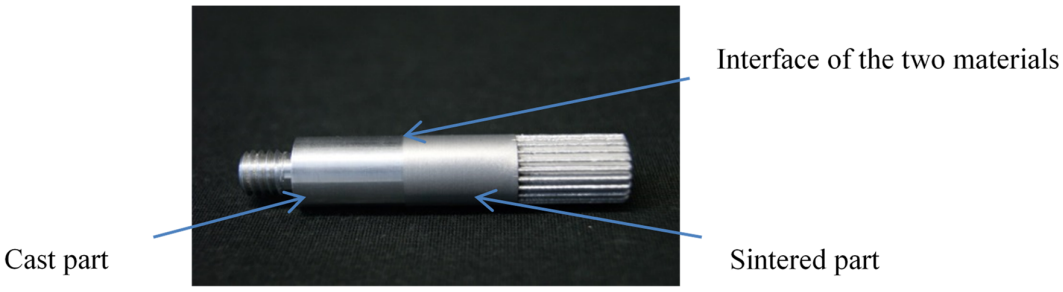

Figure 10. Hybrid printed shaft with Al base material

These two models of machine elements exemplify the abilities not only to print parts directly, but also how to integrate functions that are not available by conventional manufacturing methods. This work has been carried out using more than one processing step, though manufacturing of comparable parts would require even more manufacturing steps and processing time.

7. Discussion and conclusions

Besides building standalone parts the presented approach opens the possibility to manufacture parts on top of pre-machined preforms for high efficiency not only for single or composite material objects but even for hybrid tooling.

As presented, it could be concluded that there are numerous parameters which can influence the building process and the out coming results significantly. This work revelaed that the direction of building is important to reduce part failure possibilities: it is not preferable to print in z direction for the critical load points. For instance, further research could be extended to the interface area between base part and the added printed part. This might include an adapted chamber room atmosphere, adjusting the laser parameters or layer thickness and optimizing the geometry of the contact surface by different orientations angles. In general, the process shows a good material quality with low porosity and good mechanical properties in tensile tests. Therefore, further dynamic or cyclic tests should be carried on shafts and gears to validate this process under more complex loading conditions and environments.

Furthermore, the results of the second application in this work showed a developed method able to make use of the advantage of building on top of pre-machined preforms in an additonal way. Building hollow gears and shafts by using SLM machines exemplifies the ability to build Machine Elements with internal enforcing structures while entirely solid at the outside. This can reduce the weight and the consumed material, integrate functions in parts and keep good mechanical properties all at the same time. For example, a tooth of a gear, redesigned by adding enforcing structures and re-distributing loads on the root of the tooth is an idea worth trying in case we would like to reduce the weight by removing material from the tooth inside or to integrate lubrication channels inside. Building bearings with efficient cooling and lubricating joints inside is also a challenge for traditional manufacturing methods.

It can be concluded from the tensile test that it is possible to connect volumes manufactured from different aluminum alloys without failure in the interface zone of these parts. Further studies are intended to test the tensile bond strength between a wide range of alloys from identical or different base metals to identify possible material combinations for this type of hybrid material printing.

Further studies are planned to understand how the laser power will affect the density and hardness for different zones starting from the surface to the core of the part and to reveal advantages by such an adapted processing.
Finally, it can be concluded that the presented results will enable future developments to build one piece parts of different material combinations, adapted density zones and light weight properties with internal enforcing structures by almost only one manufacturing process.

References

Agarwala, M., Bourell, D., Beaman, J., Marcus, H., Barlow, J., "Direct selective laser sintering of metals", Rapid Prototyping Journal, Vol.1, No.1, 1995, pp. 26-36.

Capello, E., Colombo, D., Previtali, B., "Repairing of sintered tools using laser cladding by wire", Journal of Materials Processing Technology, Vol.164, 2005, pp. 990-1000.

EOS, "Material data sheet for Aluminium AlSi10Mg", EOS GmbH, 2011.

EOS, "Technical Description for EOSINT M 280", EOS GmbH, 2010.

Kasperovich, G., Hausmann, J., "Improvement of fatigue resistance and ductility of TiAl6V4 processedby selective laser melting", Journal of Materials Processing Technology, Vol.220, 2015, pp. 202-214.

Kruth, J.-P., Mercelis, P., Van Vaerenbergh, J., Froyen, L., Rombouts, M., "Binding mechanisms in selective laser sintering and selective laser melting", Rapid Prototyping Journal, Vol.11, No.2, 2005, pp. 26-36.

Lachmayer, R., Lippert, R. B., Fahlbusch, T. (Eds.), "3D-Druck beleuchtet, Additive Manufacturing auf dem Weg in die Anwendung", Springer-Verlag Berlin Heidelberg, 2016.

Manfredi, D., Calignano, F., Krishnan, M., Canali, R., Ambrosio, E., Biamino, S., Ugues, D., Pavese, M., Fino, P., "Additive Manufacturing of Al Alloys and Aluminium Matrix Composites (AMCs)", Light Metal Alloys Application, InTech, 2014.

Murali, K., Chatterjee, A. N., Saha, P., Palai, R., Kumar, S., Roy, S. K., Mishra, P. K., Roy Choudhury, A., "Direct selective laser sintering of iron–graphite powder mixture", Journal of Materials Processing Technology, Vol.136, 2003, pp. 179-185.

Olakanmi, E. O., "Selective laser sintering/melting (SLS/SLM) of pure Al, Al–Mg, and Al–Si powders: Effect of processing conditions and powder properties", Journal of Materials Processing Technology, Vol.213, No.8, 2013, pp. 1387-1405.

Olakanmia, E. O., Cochranea, R. F., Dalgarnoc, K. W., "A review on selective laser sintering/melting (SLS/SLM) of aluminium alloy powders: Processing, microstructure, and properties", Progress in Materials Science, Vol.74, 2015, pp. 401-477.

Shen, W., Wang. L., Hao, Q., "Agent-based distributed manufacturing process planning and scheduling: a state-of-the-art survey", IEEE Transactions on Systems, Man, and Cybernetics, Part C (Applications and Reviews), Vol.36, No.4, 2006, pp. 563-577.

Simchi, A., Pohl, H., "Direct laser sintering of iron–graphite powder mixture", Materials Science and Engineering A, Vol.383, No.2, 2004, pp. 191-200.

Simchi, A., Pohl, H., "Effects of laser sintering processing parameters on the microstructure and densification of iron powder", Materials Science and Engineering: A, Vol.359, No.1, 2003, pp. 119-128.

Tammas-Williams, S., Zhao, H., Léonard, F., Derguti, F., Todd, I., Prangnell, P. B., "XCT analysis of the influence of melt strategies on defect population in Ti–6Al–4V components manufactured by Selective Electron Beam Melting", Materials Characterization, Vol.102, 2015, pp. 47-61.

Yousif Amsad Zghair, M. Sc. in mechanical engineering
Hannover University, ipeg institute
Welfengarten 1A, 30167 Hannover, Germany
Email: zghair@ipeg.uni-hannover.de